Estimation of Nonlinear Contributions in Human Controller Frequency Response Functions

Wagenaar, Saskia; Pool, Daan; Damveld, Herman; van Paassen, Rene; Mulder, Max

DOI
10.1109/SMC.2018.00582

Publication date
2018

Document Version
Accepted author manuscript

Published in
Proceedings of the IEEE International Conference on Systems, Man, and Cybernetics

Estimation of Nonlinear Contributions in Human Controller Frequency Response Functions

Saskia E. Wagenaar, Daan M. Pool, Herman J. Damveld, Marinus M. van Paassen and Max Mulder
Control & Simulation, Department Control & Operations
Delft University of Technology, Delft, The Netherlands
Email (corresponding author): d.m.pool@tudelft.nl

***Abstract*—Traditional Frequency Response Function (FRF) estimation techniques used for analysis of Human Controller (HC) dynamics in tracking tasks assume HC dynamics to be linear, but generally do not quantify or compensate for the effects of human nonlinearities. The robust and fast Best Linear Approximation (BLA) techniques for estimating an FRF do provide such quantification of nonlinear distortions caused by Period-In-Same-Period-Out (PISPO) nonlinearities and can reduce the effect of PISPO nonlinear operations on the FRF estimate. This paper investigates the application of these BLA techniques to both measured and simulated HC data. For the simulated data, a linear HC model was deliberately extended with a symmetric PISPO deadzone nonlinear operator and a realistic level of HC "remnant" noise. Overall, both the measured and the simulated data indicate that due to the high levels of remnant noise inherent to HC data, no consistent estimate of PISPO nonlinear contributions could be made. This also means that the improvement of using BLA techniques and averaging over multiple forcing function realizations does not result in a substantial improvement over the current practice of estimating HC FRFs from repeated measurements of a single forcing function.**

I. Introduction

Human controller (HC) dynamics are mostly measured in compensatory tracking tasks with quasi-random multisine forcing functions [1], [2], in which a human controller is asked to continuously minimize a tracking error presented on a visual display. HC behavior is then generally analyzed by estimating a Frequency Response Function (FRF) of HCs' control dynamics, which also serves as a reference for fitting linear HC models [1]–[3]. The part of the measured control responses that cannot be explained by a linear model is the HC "*remnant*", which includes all nonlinear operations, non-steady and time-varying behavior and pure noise injected by the HC [1], [4]. To reduce the effects of remnant on estimates of HC FRFs, it is common practice to collect repeated measurements (with the same forcing functions) to average out the remnant contribution. The specific impact of individual nonlinear contributions on the estimated FRFs has, however, not yet been explicitly considered.

The Best Linear Approximation (BLA) measurement approach [5] has been developed to obtain the best possible FRF estimate of weakly nonlinear systems operating in a closed loop. By using clever data-averaging techniques, which are implemented differently for the *robust* and *fast* BLA methods [5], this approach not only reduces the impact of nonlinear operators on the FRF estimate, but also provides explicit insight into how large the impact of nonlinear contributions on the FRF estimate actually is. While the fast method, equivalent to the traditional approach to HC FRF estimation, only uses repeated measurements of a single forcing function, the robust method also uses different *realizations* of multisine forcing functions (by changing the phases of the sinusoids) to improve its estimates. While not yet applied to estimating HC FRFs, these BLA measurement approaches have been successfully applied to analyze other weakly nonlinear systems operating in a closed loop [6]–[8].

The goal of this paper is twofold. First, the robust and fast BLA measurement procedures [5] will be used to investigate whether conventional FRF estimation techniques for HC control behavior can be improved using these methods. Second, it will be investigated whether these methods can also be used for estimating the level of nonlinear contributions in typical HC data, and thereby learn more about the possible nonlinear HC dynamics that are generally simply lumped into the "remnant". To achieve these goals, both measured and simulated HC data are analyzed in this paper, for a compensatory tracking task with double integrator controlled system dynamics. For the simulation data, a quasi-linear HC model is used, with parameters tuned to match the experiment data. Furthermore, a symmetric nonlinear deadzone operator is added to the simulation to account for typical nonlinear HC dynamics [9]. The extent to which the level and nature of this nonlinear contribution can be retrieved from HC control data will then be used to determine the effectiveness of the BLA techniques for our application.

II. Human Operator Manual Control

A. Control Task

A typical manual compensatory tracking task is depicted in Fig. 1. Such tasks involve the continuous minimization of a tracking error from a visual display. The input to the human controller (HC), $i(t)$, is this tracking error, and the HC's output is the control input $y(t)$ that is applied to the controlled element (CE) H_c. In tracking tasks, errors to be corrected by the HC are typically induced using a target forcing function, $f_t(t)$, that defines the reference the HC is instructed to follow. Most research into HC compensatory control behavior uses quasi-random multisine signals for the target forcing function [1], [2], [10].

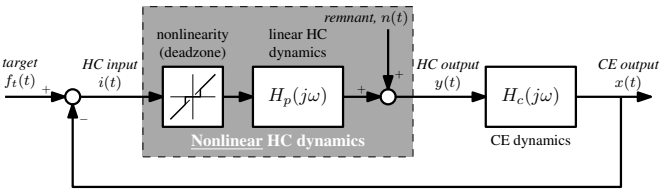

Fig. 1. Schematic representation of a compensatory tracking task.

B. Human Controller Dynamics

It is well-known that HC dynamics in compensatory tasks are quasi-linear [1]. Hence, compensatory HC models generally consist of a linear HC describing function $H_p(j\omega)$ and a remnant signal $n(t)$ that accounts for all nonlinear contributions not captured by the linear model [1], see Fig. 1. The linear HC dynamics $H_p(j\omega)$ are known to be modeled accurately with models of the form of [1], [2]:

$$\begin{aligned} H_p(j\omega) &= K_p \left(\frac{T_L j\omega + 1}{T_I j\omega + 1}\right) e^{-j\omega\tau_p} H_{nm}(j\omega) \\ H_{nm}(j\omega) &= \frac{\omega_{nm}^2}{(j\omega^2) + 2\zeta_{nm}\omega_{nm} j\omega + \omega_{nm}^2} \end{aligned} \tag{1}$$

In (1), K_p is the HC gain, T_L and T_I are the HC's lead and lag time constants, and τ_p is the HC delay. The dynamics of the neuromuscular system are typically included as a second-order mass-spring-damper model with natural frequency ω_{nm} and damping ratio ζ_{nm} [1], [2].

Contributions to the remnant $n(t)$ include nonlinear operations, non-steady and time-varying control behavior and pure noise injected by the operator [1], [4]. Generally, HC remnant is modeled as colored (low-pass filtered) white noise with an intensity that is roughly proportional to the power of the HC control signal, $y(t)$ [4], [11]. In this paper, a second-order low-pass filter – with a remnant gain K_n and time constant T_n as the parameters – is used for modeling the remnant:

$$H_n(j\omega) = \frac{K_n}{(T_n j\omega + 1)^2} \tag{2}$$

Note that this approach to modeling HC remnant lumps all nonlinear, time-varying and noise-injection processes together and thus does not explicitly distinguish between the different nonlinear contributions to the (linear time-invariant) remnant.

III. Frequency Response Function Estimation

A. Traditional HC FRF Estimation

To estimate the linear HC describing function $H_p(j\omega)$, see Fig. 1, traditionally an HC FRF is estimated using the instrumental variable approach enabled by the use of a multisine forcing function $f_t(t)$ [1]–[3]:

$$\hat{H}_p(j\omega_k) = \frac{\hat{S}_{yf_t}(j\omega_k)}{\hat{S}_{if_t}(j\omega_k)} \tag{3}$$

In (3), $\hat{S}_{yf_t}(j\omega_k)$ and $\hat{S}_{if_t}(j\omega_k)$ are the cross-power spectral density estimates of the HC output $y(t)$ and input $i(t)$ with the forcing function $f_t(t)$ at the k^{th} frequency excited by the forcing function, ω_k. Due to the feedback of the remnant noise in the closed-loop system and other HC nonlinearities, an FRF estimated with (3) is generally biased, with a bias that can be explicitly determined [3]. Generally, this is countered by collecting multiple (e.g., five to ten [1], [10]) repeated measurements and averaging the time- ($i(t)$ and $y(t)$) or frequency-domain ($\hat{S}_{yf_t}(j\omega_k)$ and $\hat{S}_{if_t}(j\omega_k)$) data.

B. Best Linear Approximation

The BLA is an optimal linear approximation of the dynamics of weakly nonlinear systems that minimizes the mean square error between the outputs of the true nonlinear system and its linear FRF [5], [12], [13]. BLA techniques rely on smart forcing function design and controlled data-averaging techniques – both over repeated period measurements P and varying phase realizations M of the applied multisine signals – to obtain improved FRF estimates. With this approach, also the impact of Period-In-Same-Period-Out (PISPO) nonlinear contributions on the FRF estimate can be explicitly quantified and minimized. For example, when a purely *odd* input signal, in which only odd integer multiples of the fundamental measurement frequency are excited, is used, the effects of odd and even nonlinear operators in the identified system can be separated: all odd (excited) frequencies are only disturbed by odd operations, while the even (unexcited) frequencies are only disturbed by even nonlinearities. This fact is exploited in this paper, as the symmetric deadzone considered as the nonlinearity in our HC dynamics is a purely odd operator.

For closed-loop BLA techniques, generally a distinction is made between two different methods. The *robust method* uses both multiple measurements using different multisine signals (M) and several periods of the same multisine signals (P) to determine, and average out, the effects of nonlinear operators and stochastic measurement noise. The *fast method* only requires repetitions of one forcing function (P), but an approximation is needed to estimate the noise and stochastic nonlinear distortions on the FRF [5]. In general it is recommended to use $P \geq 4$ repetitions with the fast method, while $P \geq 2$ repetitions and $M \geq 4$ phase realizations, and thus more data, are generally required for the robust method [5].

1) FRF Estimation: To estimate an improved FRF, both the fast and robust BLA methods use an average of the HC input signal $I(j\omega_k)$ and HC output signal $Y(j\omega_k)$ at the frequencies excited by $f_t(t)$, calculated over a number of repeated periods P of each forcing function realization (m), according to:

$$\hat{I}^{[m]}(j\omega_k) = \frac{1}{P}\sum_{p=1}^{P} I^{[m,p]}(j\omega_k) \tag{4}$$

In (4), the superscripts between square brackets indicate the dependency of the signal on different realizations of $f_t(t)$, m, and on repeated period measurements p. The same equation as (4) is also used to calculate the averaged HC output, $\hat{Y}^{[m]}(j\omega_k)$. The BLA is then calculated by further averaging of $\hat{I}^{[m]}(j\omega_k)$ and $\hat{Y}^{[m]}(j\omega_k)$ over the phase realizations M,

TABLE I
FORCING FUNCTION FREQUENCIES, AMPLITUDES AND PHASES.

k (-)	n_k (-)	ω_k (rad/s)	A_k (inch)	$\phi_{k,1}$ (rad)	$\phi_{k,2}$ (rad)	$\phi_{k,3}$ (rad)	$\phi_{k,4}$ (rad)	$\phi_{k,5}$ (rad)	$\phi_{k,6}$ (rad)	$\phi_{k,7}$ (rad)	$\phi_{k,8}$ (rad)	$\phi_{k,9}$ (rad)	$\phi_{k,10}$ (rad)
1	1	0.10	0.288	2.901	4.419	1.273	3.373	2.722	5.380	5.243	2.049	4.514	2.914
2	3	0.30	0.288	4.090	3.301	4.102	3.207	0.694	3.143	0.279	5.411	5.125	5.924
3	5	0.50	0.288	1.745	1.837	3.172	4.385	5.781	0.898	3.116	5.722	1.990	1.777
4	7	0.71	0.288	5.591	4.774	6.067	4.949	5.331	2.881	2.209	2.313	3.095	1.327
5	9	0.91	0.288	0.276	0.140	3.150	1.466	2.618	5.814	2.787	1.854	0.397	1.549
6	15	1.51	0.288	3.852	1.111	5.491	0.461	0.766	5.019	1.762	5.453	5.913	0.800
7	25	2.52	0.029	2.113	5.462	1.330	1.170	5.978	4.087	3.994	3.632	0.233	3.550
8	41	4.13	0.029	2.529	1.263	1.691	1.777	1.089	5.127	2.397	3.162	6.037	4.913
9	75	7.56	0.029	3.966	0.043	5.598	2.731	3.084	0.042	0.419	0.607	3.662	0.355
10	135	13.61	0.029	4.761	5.696	0.727	6.001	4.562	2.826	4.921	3.255	5.457	5.234

taking care of compensating for the different phases of the input signals at the input frequencies, $\angle F_t^{[m]}(j\omega_k)$:

$$\hat{G}_{BLA}(j\omega_k) = \frac{\frac{1}{M}\sum_{m=1}^{M} \hat{Y}^{[m]}(j\omega_k)e^{-j\angle F_t^{[m]}(j\omega_k)}}{\frac{1}{M}\sum_{m=1}^{M} \hat{I}^{[m]}(j\omega_k)e^{-j\angle F_t^{[m]}(j\omega_k)}} \quad (5)$$

Note that as for the fast method $M = 1$, this second averaging is only performed with the robust method.

2) Nonlinear and Noise Contributions: In addition to providing an estimate of the BLA of a weakly nonlinear system, the BLA measurement techniques also provide an estimate of both the level of nonlinear contributions and noise from other sources. The estimated BLA, $\hat{G}_{BLA}(j\omega_k)$, is thus the sum of the true BLA of the nonlinear system, stochastic contributions of nonlinear operators $G_S(j\omega_k)$, and the contributions of measurement noise $N_G(j\omega_k)$:

$$\hat{G}_{BLA}(j\omega_k) = G_{BLA}(j\omega_k) + G_S(j\omega_k) + N_G(j\omega_k) \quad (6)$$

The use of repeated measurements P and different realizations M allows for estimating the contributions of $G_S(j\omega_k)$ and $N_G(j\omega_k)$ to the estimated BLA. The variance of the noise contribution, here referred to as $\hat{\sigma}^2_{\hat{G}_{BLA},n}$, is estimated from the sample variance of the FRF estimates over the periods P only, with averaging this variance estimate over the phase realizations M (robust method), see (7). Since PISPO nonlinearities have a constant contribution for each period, the nonlinear contributions do not affect this sample variance.

$$\hat{\sigma}^2_{\hat{G}_{BLA},n}(j\omega_k) = \frac{\hat{\sigma}^2\{N_G(j\omega_k)\}}{MP} \quad (7)$$

$$\hat{\sigma}^2_{\hat{G}_{BLA}}(j\omega_k) = \frac{\hat{\sigma}^2\{G_S(j\omega_k)\}}{M} + \frac{\hat{\sigma}^2\{N_G(j\omega_k)\}}{MP} \quad (8)$$

Similarly, when computing the variance of estimated FRFs over the different phase realizations M, the stochastic nonlinear contributions do vary, and contribute to the variance estimate. Consequently, a total variance of the BLA ($\hat{\sigma}^2_{\hat{G}_{BLA}}$) is obtained, see (8), including both variance introduced by $G_S(j\omega_k)$ and $N_G(j\omega_k)$. The difference between the estimated noise variance and total variance thus provides a direct estimate of the contribution of the nonlinear distortions, $G_S(j\omega_k)$.

With (7) and (8), the nonlinear and noise contributions to the estimated FRF can be estimated at the excited measurement frequencies ω_k. Following the same rationale, also the variability due to noise and nonlinear system operators *at all frequencies* can be separated over the different measurements of the system output signal [5], here $Y^{[m,p]}(j\omega)$. In this paper, both the variability in the BLA ($\hat{\sigma}^2_{\hat{G}_{BLA}}$ and $\hat{\sigma}^2_{\hat{G}_{BLA,n}}$) and in the HC output ($\hat{\sigma}^2_{\hat{Y}}$ and $\hat{\sigma}^2_{\hat{Y},n}$) are analyzed to verify the extent to which nonlinear distortions can be estimated from HC data.

IV. EXPERIMENT

A. Experiment Setup

1) Control Task and Apparatus: For this paper, experiment data were collected from one participant, who performed a compensatory tracking task as shown in Fig. 1. The experiment was performed in the part-task simulator setup of the Human-Machine Interaction Laboratory at the Faculty of Aerospace Engineering at TU Delft. The CE dynamics were a double integrator, $H_c(s) = K_c/s^2$, with $K_c = 5$. The participant controlled the CE with a passive side-stick, with characteristics equal to those reported in [14].

2) Forcing Functions: The forcing functions for the experiment were traditional random-appearing multisine signals with a high-frequency shelf amplitude distribution [1], [10]:

$$f(t) = \sum_{k=1}^{N} A_k \sin(\omega_k t + \phi_k) \text{ with } \omega_k = \frac{2\pi n_k}{T} \quad (9)$$

In (9), N indicates the total number of sinusoids, ω_k the excited frequencies, and ϕ_k and A_k the phase shift and the amplitude of each sinusoid, respectively. To prevent leakage in the Fourier signal analysis and to ensure that an estimate of even and uneven nonlinear contributions could be made, the sinusoid frequencies ω_k were chosen as *odd* integer multiples of the base frequency $2\pi/T$. The measurement period T for this experiment was chosen to be 62.3 seconds. The amplitudes were uniformly scaled to have a standard deviation of f_t equal to 0.5 inch.

To enable application of both the robust and the fast methods, data were collected for $M = 10$ phase realizations

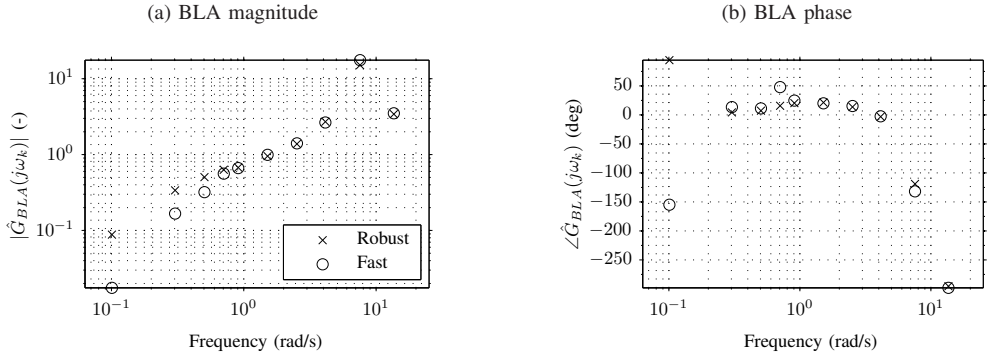

Fig. 2. Estimated BLA of the HC dynamics for the robust and fast methods (M = 10 and P = 6).

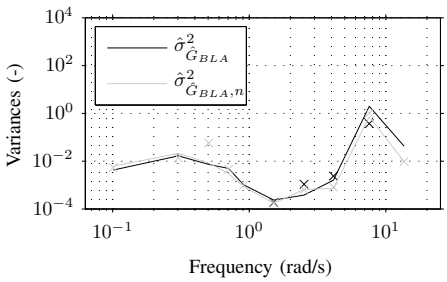

Fig. 3. Total and noise variance on the BLA for the robust (lines) and fast (crosses) methods (M = 10 and P = 6).

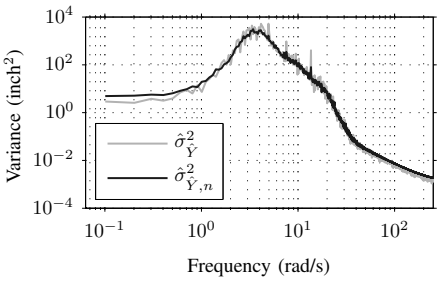

Fig. 4. Total and noise variance on the HC output signal $y(t)$ for the robust method (M = 10 and P = 6).

ϕ_k, each for 6 repeated period measurements P. The ϕ_k were selected from a pool of randomly-generated phase sets according to the procedure described in [10]. The used sinusoid frequencies, amplitudes, and phases are listed in Table I.

B. Experiment Results

Fig. 2 shows the FRFs of the BLA $\hat{G}_{BLA}(j\omega_k)$ of the HC dynamics as estimated with both the robust and fast methods. For the fast method, the result for one of the phase realizations is shown, which is equivalent to a traditional HC FRF estimate [1]. As is clear from Fig. 2, both methods give equivalent results, especially at the higher excited frequencies. At low frequencies, fewer repeated periods of the sinusoids are available over the measurement time. In addition, for the considered task with a double integrator CE, the HC control dynamics also have low magnitude at the low frequencies, see Fig. 2. These effects explain the larger differences between both methods for the lower excited frequencies, where the robust method BLA is in general more accurate due to the additional averaging over the phase realization M.

Fig. 3 shows the estimated variance of the BLA, both the total variance (gray data) and the variance attributed to noise (black data) for the robust (lines) and fast (crosses) methods. For the fast method, these variances could only be estimated for the four highest frequencies, as with the chosen measurement time and the required odd input frequencies it was not possible to leave odd frequencies unexcited in this frequency range, see Table I. As is evident from Fig. 3, only very small differences between the total and noise variances of $\hat{G}_{BLA}(j\omega_k)$ are observed, which indicates that no significant contributions of possible PISPO nonlinearities could be measured at the excited frequencies.

The same can be concluded from a comparison of the total and noise variance components present in the measured HC output signals $y(t)$. Fig. 4 shows the estimated variance in $y(t)$ at *all* (i.e., both excited and unexcited) frequencies for the robust method only, as the variance estimates for the fast method were equivalent. As is evident from Fig. 4, also in the HC output and over the whole frequency range covered by the measurement the total and noise variance estimates are equivalent, and thus no strong indication of the presence of PISPO nonlinear contributions is found.

V. Simulations

A. Simulation Setup

1) Human Controller Model: The simulations were setup to match the experiment data, to allow for a fair comparison of the results. In the simulations the HC dynamics $H_p(j\omega)$ were represented by the HC model of (1). The model parameters were tuned based on the collected experiment data, estimating them from these data with the time-domain procedure of [15]. The estimated model fits to the data from the M = 10 phase realizations had an average Variance Accounted For (VAF) of 90.5% and resulted in average parameter estimates of K_p = 0.61, T_L = 0.74 s, τ_p = 0.27 s, ω_{nm} = 7.76 rad/s, and ζ_{nm} = 0.13. Remnant intensity and frequency characteristics were similarly estimated from the experiment data, resulting in K_n = 0.6 and T_n = 0.1 s to be used with the model of (2).

2) PISPO Nonlinear HC Dynamics: For the simulation analysis, an PISPO nonlinear deadzone (DZ) operator was

included in the HC dynamics model, as shown in Fig. 1. The DZ is a symmetric threshold-like operator that is likely to occur in HC dynamics [1], [9] and here is assumed to work on the HC input signal $i(t)$, to model an HC who only responds to tracking errors that are above a certain magnitude. The DZ threshold was set to 0.05 inch, which is around 10% of the highest peak of the error signal.

3) Forcing Functions: The forcing functions were chosen to directly match the measurement case, as described in Section IV-A2, with $M = 10$ phase realizations and $P = 6$ repeated period measurements. To assess the stochastic variability in the results, all simulation data were generated for 100 different realizations of the simulated remnant noise.

4) Simulation Cases: To verify the extent to which PISPO nonlinear contributions from the considered threshold operator could be estimated from simulated HC data, four simulation cases were considered, as listed in Table II. The CLEAN and DZ cases were included to verify the known performance of the robust and fast methods on noise-free data [5]. For the DZ case, the pure PISPO nonlinear contributions on the FRF estimation process will be quantified. For the DZ+REM case additional modeled HC remnant noise is added to the simulation data, as is also present on real HC data. Finally, the REM condition is included for quantifying the effects of remnant on the estimation results, for comparison to the DZ+REM data.

TABLE II
SUMMARY OF SIMULATION CASES.

	No Deadzone	With Deadzone
No Remnant	CLEAN	DZ
With Remnant	REM	DZ+REM

B. Simulation Results

Matching the corresponding experiment data presented in Fig. 3 and 4, Fig. 5 and 6 show the estimated total (black) and noise (gray) variances on the BLA FRF estimate and the HC output signal $y(t)$, respectively, for the four simulation cases listed in Table II. The results presented in Fig. 5 for the fast (crosses) and robust (lines) methods are averaged over 100 different remnant realizations. Fig. 6 only presents results of the robust method, which for the REM and DZ+REM cases also shows the spread in the obtained results with a shaded area matching the 5^{th} and 95^{th} percentiles.

For the CLEAN, DZ, and REM simulation cases, the expected results are obtained. For the CLEAN case, see Fig. 5a and 6a, both the total and noise variances are negligible due to the absence of both nonlinearities and remnant. The gaps between the data points in Fig. 6a are caused by estimated values truly equal to zero, which cannot be represented on a logarithmic scale. For simulation case DZ (Fig. 5b and 6b), only a substantial variance due to the DZ is found, together with a negligible noise contribution. Fig. 6b also clearly shows the nature of the odd deadzone operator, which with the used odd input signal only shows a contribution at odd measurement frequencies. Finally, Fig. 5c and 6c show that for the REM case the total and noise variances are substantial and nearly overlap, which is expected in the absence of additional nonlinearities.

For the DZ+REM case, Fig. 5d and 6d show results equivalent to those obtained for the REM case. Thus, despite the fact that a pure PISPO nonlinear operator is present in the control loop, its effects on the total variances of the BLA estimate and the HC output signal are negligible. This shows that with significant additional (remnant) noise, as is characteristic of all HC data [1], [2], it is not possible to detect the presence of PISPO nonlinear operators, such as a deadzone, using the techniques considered in this paper.

VI. CONCLUSION

The robust and fast Best Linear Approximation (BLA) techniques for estimating Frequency Response Functions (FRF) of nonlinear systems were applied to measured and simulated data of human controllers' (HC) compensatory control behavior. The main goal was to investigate if more reliable FRF estimates were obtained than with conventional FRF estimation techniques for HC behavior and if explicit estimates of typical nonlinear Period-In-Same-Period-Out (PISPO) contributions, such as a deadzone (DZ) operator at the HC input, could be obtained. Overall, it is concluded that when typical HC remnant noise from other sources than PISPO nonlinearities is present, the current practice of estimating the FRF from repeated measurements of one forcing function is as effective as averaging over various forcing function realizations, as done in the robust method. Furthermore, due to the high noise level of typical HC data, both the measured and the simulated data indicate that no consistent estimate of the presence of PISPO nonlinearities such as a DZ can be obtained from measured HC control behavior with the considered methods.

REFERENCES

[1] D. T. McRuer and H. R. Jex, "A Review of Quasi-Linear Pilot Models," *IEEE Trans. on Human Factors in Electronics*, vol. HFE-8, no. 3, pp. 231–249, 1967.

[2] M. Mulder, D. M. Pool, D. A. Abbink, E. R. Boer, P. M. T. Zaal, F. M. Drop, K. van der El, and M. M. van Paassen, "Manual Control Cybernetics: State-of-the-Art and Current Trends," *IEEE Trans. on Human-Machine Systems*, 2018.

[3] A. van Lunteren, "Identification of Human Operator Describing Function Models with One or Two Inputs in Closed Loop Systems," Ph.D. dissertation, Delft University of Technology, Faculty of Mechanical Engineering, 1979.

[4] W. H. Levison, S. Baron, and D. L. Kleinman, "A Model for Human Controller Remnant," *IEEE Trans. on Man-Machine Systems*, vol. 10, no. 4, pp. 101–108, 1969.

[5] R. Pintelon and J. Schoukens, "FRF Measurement of Nonlinear Systems Operating in Closed Loop," *IEEE Trans. On Instrumentation and Measurement*, vol. 62, no. 5, pp. 1334–1345, 2013.

[6] R. Pintelon, Y. Rolain, G. Vandersteen, and J. Schoukens, "Experimental Characterization of Operational Amplifiers: A System Identification Approach – Part II: Calibration and Measurements," *IEEE Trans. on Instrumentation and Measurement*, vol. 53, no. 3, pp. 863–876, 2004.

[7] E. Wernholt and S. Gunnarsson, "Estimation of Nonlinear Effects in Frequency Domain Identification of Industrial Robots," *IEEE Trans. on Instrumentation and Measurement*, vol. 57, no. 4, pp. 856–863, 2008.

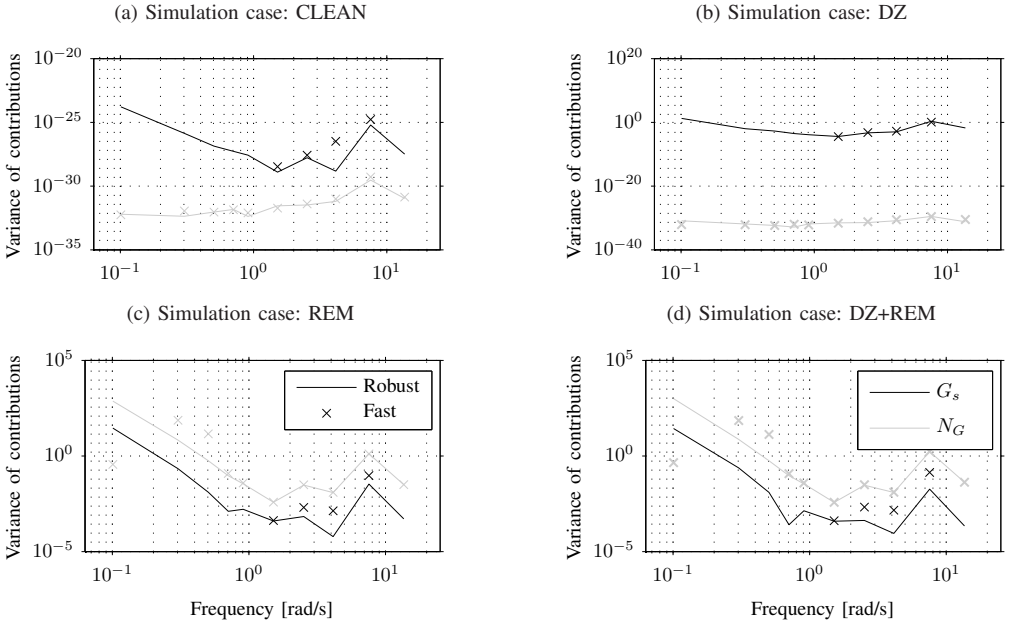

Fig. 5. Total and noise variances of the BLA estimate averaged over 100 simulations, with $P = 6$ and $M = 10$.

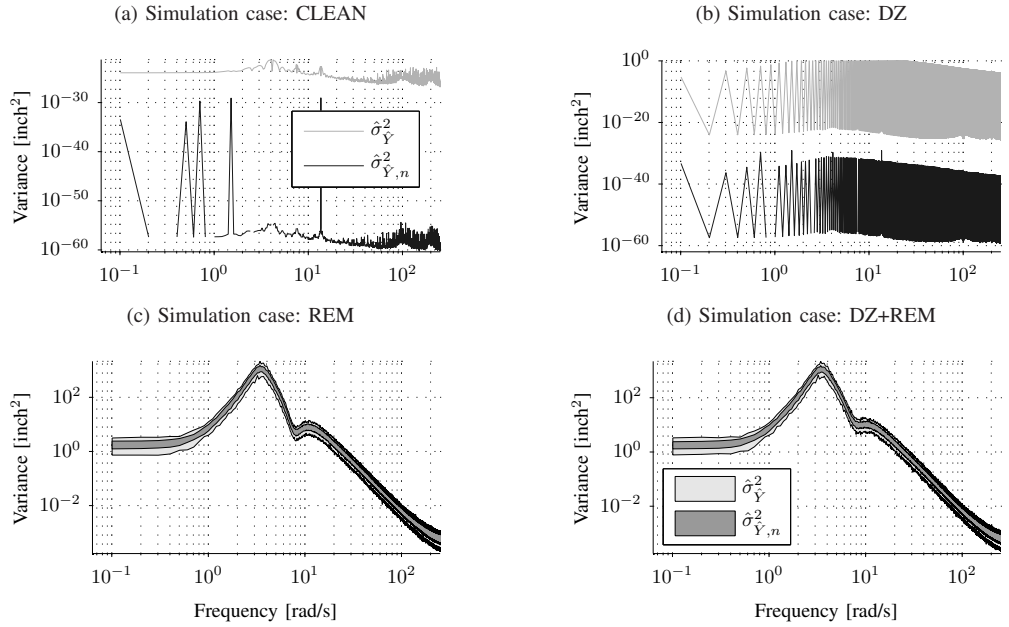

Fig. 6. Simulated noise and total variance for four different simulation cases, with $P = 6$ and $M = 10$ for 100 repeated simulations.

[8] L. De Locht, G. Vandersteen, Y. Rolain, and R. Pintelon, "Estimating Parameterized Scalable Models From the Best Linear Approximation of Nonlinear Systems for Accurate High-Level Simulations," *IEEE Trans. on Instr. and Measurement*, vol. 55, no. 4, pp. 1186–1191, 2006.

[9] A. R. Valente Pais, D. M. Pool, A. M. de Vroome, M. M. van Paassen, and M. Mulder, "Pitch Motion Perception Thresholds During Passive and Active Tasks," *Journal of Guidance, Control, and Dynamics*, vol. 35, no. 3, pp. 904–918, 2012.

[10] H. J. Damveld, G. C. Beerens, M. M. van Paassen, and M. Mulder, "Design of Forcing Functions for the Identification of Human Control Behavior," *Journal of Guidance, Control, and Dynamics*, vol. 33, no. 4, pp. 1064–1081, 2010.

[11] H. R. Jex and R. E. Magdaleno, "Corroborative Data on Normalization of Human Operator Remnant," *IEEE Trans. on Man-Machine Systems*, vol. 10, no. 4, pp. 137–140, 1969.

[12] J. Schoukens, T. Dobrowiecki, and R. Pintelon, "Parametric and Non-parametric Identification of Linear Systems in the Presence of Nonlinear Distortions – A Frequency Domain Approach," *IEEE Trans. on Automatic Control*, vol. 43, no. 2, pp. 176–190, 1998.

[13] R. Pintelon and J. Schoukens, "Measurement and Modelling of Linear Systems in the Presence of Non-Linear Distortions," *Mechanical Systems and Signal Processing*, vol. 16, no. 5, pp. 785–801, 2002.

[14] K. van der El, D. M. Pool, H. J. Damveld, M. M. van Paassen, and M. Mulder, "An Empirical Human Controller Model for Preview Tracking Tasks," *IEEE Trans. on Cybernetics*, vol. 46, no. 11, pp. 2609–2621, 2016.

[15] P. M. T. Zaal, D. M. Pool, Q. P. Chu, M. M. van Paassen, M. Mulder, and J. A. Mulder, "Modeling Human Multimodal Perception and Control Using Genetic Maximum Likelihood Estimation," *Journal of Guidance, Control, and Dynamics*, vol. 32, no. 4, pp. 1089–1099, 2009.